Atomistic Simulations of fcc $Pt_{75}Ni_{25}$ and $Pt_{75}Re_{25}$ Cubo-octahedral Nanoparticles

Guofeng Wang [1], M.A. Van Hove [1,2,3], P.N. Ross [1], and M.I. Baskes [4]
[1] Materials Sciences Division, Lawrence Berkeley National Laboratory, University of California, Berkeley, CA 94720
[2] Advanced Light Source, Lawrence Berkeley National Laboratory, University of California, Berkeley, CA 94720
[3] Department of Physics, University of California, Davis, CA 95616
[4] MST-8 Structure and Property Relations Group, Los Alamos National Laboratory, Los Alamos, NM 87545

ABSTRACT

We have developed interatomic potentials for Pt-Ni and Pt-Re alloys within the modified embedded atom method (MEAM). Furthermore, we applied these potentials to study the equilibrium structures of $Pt_{75}Ni_{25}$ and $Pt_{75}Re_{25}$ nanoparticles at T=600 K using the Monte Carlo method. In this work, the nanoparticles are assumed to have disordered fcc cubo-octahedral shapes (terminated by {111} and {100} facets) and contain from 586 to 4033 atoms (corresponding to a diameter from 2.5 to 5 nm). It was found that, due to surface segregation, (1) the $Pt_{75}Ni_{25}$ nanoparticles form a surface-sandwich structure: the Pt atoms are enriched in the outermost and third atomic shells, while the Ni atoms are enriched in the second atomic shell; (2) the equilibrium $Pt_{75}Re_{25}$ nanoparticles adopt a core-shell structure: a Pt-enriched shell surrounding a Pt-deficient core.

INTRODUCTION

Developing low-cost yet high-performance electrodes is a major thrust in fuel cell research. In the past years, considerable progress has been made in characterizing and understanding the catalytic properties of Pt and Pt-bimetallic bulk alloy surfaces [1]. Due to high surface-volume ratio, Pt and Pt-bimetallic nanoparticles can perform better than thin films as electro-catalysts in lower temperature polymer electrolyte fuel cells. Since Pt is a precious active catalyst with a wide range of applications, it is highly desirable to design catalyst nanoparticles in which the Pt atoms are arranged predominantly at the outer surfaces. Complementary to experimental techniques, atomistic simulations can provide much insight into the equilibrium structures of nanoparticles in the nanoscale level and is the approach we take in this work.

We chose to investigate Pt-Ni and Pt-Re nanoparticles, because Pt-Ni and Pt-Re alloys are currently under experimental scrutiny and also represent two different types of surface segregation in bimetallic alloys. In the (111) and (100) surfaces of Pt-Ni alloys, the Pt atoms will be enriched in the first and third atomic layers while the Ni atoms are enriched in the second atomic layer. In contrast, the concentrations of Pt atoms will be highest in the outermost layer of Pt-Re surfaces and decrease gradually deeper inside the bulk. Moreover, Pt-Ni is an fcc-fcc bimetallic alloy, while Pt-Re is an fcc-hcp bimetallic alloy. It is quite challenging to develop a generic model to describe both systems. Baskes [2,3] solved this problem by adding directional bonding to the original embedded-atom method (EAM) [4], thus developing the modified embedded atom method (MEAM) for these kinds of metals.

SIMULATION METHODS

The detailed description of the MEAM formalism and parameters adopted in this work will be published elsewhere [5,6]. The MEAM potentials for pure fcc Pt, fcc Ni, and hcp Re were developed using empirical data for the cohesive energy, the lattice constants, the elastic constants, and the vacancy formation energy. To determine the cross potentials between Pt and Ni (or Re), we chose the intermetallic compound Pt_3Ni (or Pt_3Re), which has the $L1_2$ structure, as the reference structure. We further fit the MEAM cross potentials to first-principles calculation results of the lattice parameter, cohesive energy, and three elastic constants for Pt_3Ni (or Pt_3Re). The transferability of these potentials is checked by comparing the MEAM and first-principles results of the lattice constants and cohesive for other compounds such as $PtNi_3$ ($L1_2$), PtNi ($L1_0$), and $PtRe_3$ ($L1_2$). More importantly, these potentials lead to surface segregation profiles (concentration of Pt atoms in the different layers of surfaces) that agree quantitatively with experimental measurements.

In this work, we used a Monte Carlo (MC) method based on the Metropolis algorithm: starting from some atomic configuration, the successive configurations are generated in proportion to the probabilities of a configuration occurring in the equilibrium ensemble. In each MC step, one of the following two configuration transformations is tried out with an equal probability: (1) a randomly selected atom is displaced from its original position in a random direction. The magnitude of the displacement is in the range of $(0, r_{max}]$. At the simulation temperature, the maximum displacement r_{max} is tuned so that the acceptance rate of new configurations is about 0.5 during the equilibrated part of the simulations; and (2) two randomly selected atoms with different element types are exchanged. The new configuration is always accepted if the transformation decreases energy. When the transformation increases energy, the new configuration is accepted with a probability of $\exp(-\Delta E/kT)$, where ΔE is the energy change for the configuration transformation, k is the Boltzmann constant, and T is the simulation temperature.

RESULTS

Cubo-octahedral nanoparticles

We assumed the fcc cubo-octahedral shape (terminated by {111} and {100} facets, shown in Figure 1) for $Pt_{75}Ni_{25}$ and $Pt_{75}Re_{25}$ nanoparticles. This shape is believed to be the equilibrium shape for fcc nanoparticles from the macroscopic view of single crystal surface energy. Based on the number and arrangement of their nearest neighbors (nn), we can distinguish atoms in the nanoparticle core or surface regions: atoms have 12nn in the core and less than 12nn in the surface. Following the same procedure, we can further distinguish atoms at various sites (facet, edge and vertex) in the surface of the nanoparticles. As marked in Figure 1 using different numbers, in a cubo-octahedral nanoparticle there are: 1. twenty-four vertices (6nn), 2. twelve {111}/{111} edges (7nn), 3. twenty-four {111}/{100} edges (7nn), 4. six {100} facets (8nn), and 5. eight {111} facets (9nn). To study the size effect on segregation in nanoparticles, we chose sequences of "magic" numbers of atoms (i.e., nanoparticles containing complete shells of atoms): 586, 1289, 2406, and 4033. The diameter of these nanoparticles ranges from 2.5 to 5 nm.

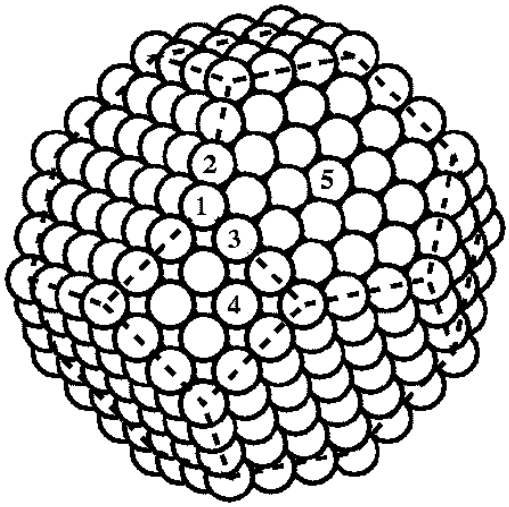

Figure 1. A fcc cubo-octahedral nanoparticle containing 586 atoms.

Equilibrium structures of nanoparticles

In an fcc lattice, the atomic sizes of Pt and Re atoms are nearly equal while the atomic sizes of Pt and Ni atoms are quite different. Therefore, more MC steps are required for the $Pt_{75}Ni_{25}$ nanoparticles than the $Pt_{75}Re_{25}$ nanoparticles to reach their equilibrium configurations. In this work, we performed MC simulations at T=600 K allowing both atomic displacement and exchange of element types up to 40 million MC steps for each $Pt_{75}Ni_{25}$ nanoparticle and 20 million MC steps for each $Pt_{75}Re_{25}$ nanoparticle. The simulation temperature T=600 K corresponds to the experimental reduction temperature used in preparing these catalyst nanoparticles. The nanoparticles initially had the lattice constants determined for the bulk alloys at the same composition and temperature 600 K with randomly distributed Pt and Ni (or Re) atoms. During the MC simulations, both the lattice constants and the distribution of the atoms in the nanoparticles change.

Figure 2 and Figure 3 show the equilibrium structures and [001] cross-sections that expose the center of the $Pt_{75}Ni_{25}$ and $Pt_{75}Re_{25}$ cubo-octahedral nanoparticles. First, both figures show a distinct "rounding" of the nanoparticles due to larger inward relaxations at the vertices and edges compared to the rest of the facets. Second, we also found that a {100}-facet reconstruction process occurs in both nanoparticles, shown in Figure 2(a) and Figure 3(a). In this process, the top layer of the {100} facets can reconstruct from a square lattice to a denser hexagonal lattice; the extra atoms needed in this process come from the core of the nanoparticles (not the surrounding edges and vertices).

Segregation profiles

Further, Figure 2 and Figure 3 indicate that the Pt and Ni (or Re) atoms are not distributed homogenously in the nanoparticles. In the $Pt_{75}Ni_{25}$ nanoparticle (Figure 2(b)), there is a higher concentration of Pt atoms (higher than 75 at.%) in the outermost and third atomic shells while a higher concentration of Ni atoms (higher than 25 at.%) is found in the second atomic shell. We name this "surface-sandwich structure" of nanoparticles. In contrast, the $Pt_{75}Re_{25}$ nanoparticle

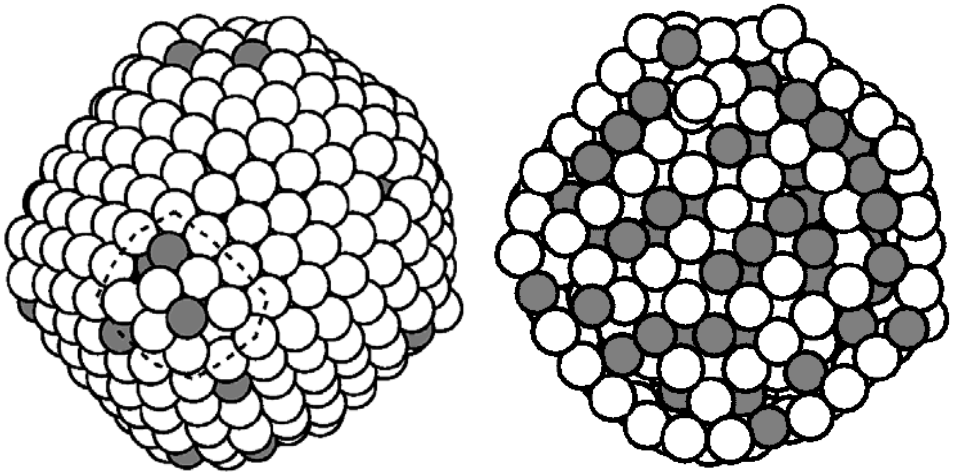

(a) **(b)**

Figure 2. (a) Snapshot and (b) [001] cross-sectional view of the equilibrium $Pt_{75}Ni_{25}$ cubo-octahedral nanoparticle containing 586 atoms, showing a surface-sandwich structure. The open and gray circles represent Pt and Ni atoms, respectively. As a guide to the eye, one reconstructed {100} facet is delineated with dashed lines in (a).

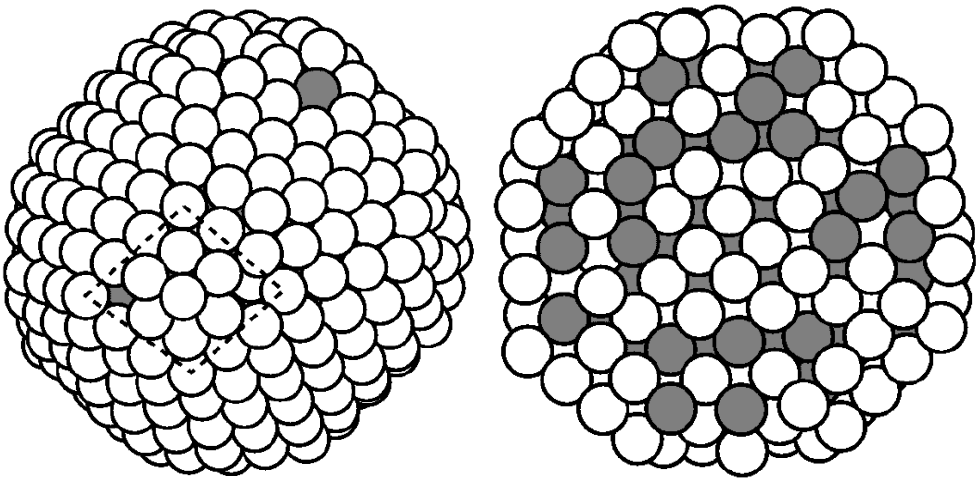

(a) **(b)**

Figure 3. (a) Snapshot and (b) [001] cross-sectional view of the equilibrium $Pt_{75}Re_{25}$ cubo-octahedral nanoparticle containing 586 atoms, showing a core-shell structure. The open, gray circles represent Pt and Re atoms, respectively. As a guide to the eye, one reconstructed {100} facet is delineated with dashed lines in (a).

has a simpler structure: the Pt atoms are enriched in the outermost shell, and are distributed more homogenously in the nanoparticle core but with a lower concentration. This is the so-called "core-shell structure" of bimetallic nanoparticles It appears that the equilibrium structures of these nanoparticles are related to their alloy surface segregation phenomena: the Pt atoms will be enriched in the first and third layers while the Ni atoms are enriched in the second layer of Pt-Ni

(111) and (100) surfaces; while the concentrations of Pt atoms will be highest in the outermost layer of Pt-Re surfaces and decrease gradually deeper inside the bulk.

We now discuss more quantitatively the concentrations of Pt atoms in the surfaces and core of nanoparticles. To eliminate the influence of the original structure, we averaged the values sampled every 10000 MC steps in the last half of whole MC simulation runs. Table I reports our results for $Pt_{75}Ni_{25}$ nanoparticles, quantitatively showing the surface-sandwich structures for the three outer layers of these nanoparticles. Table II gives corresponding results for $Pt_{75}Re_{25}$ nanoparticles, showing a core-shell structure.

It is noticed that the concentration of Pt atoms is nearly 100 at.% in the outermost layer of both $Pt_{75}Ni_{25}$ and $Pt_{75}Re_{25}$ nanoparticles. The formation of a Pt "skin" covering the core of nanoparticles is of great significance, because it guarantees a maximum exposure of active catalyst Pt to reactants. The concentrations of Pt atoms in the sub-layer (second atomic shell) of $Pt_{75}Ni_{25}$ nanoparticles are much smaller than the overall concentration of 75 at.% and increase gradually with their size. In a similar pattern, the concentrations of Pt atoms in the core (including the second layer) of $Pt_{75}Re_{25}$ nanoparticles are much smaller than the overall concentration of 75 at.% and increase gradually with their size. This implies that the Ni or Re atoms are enriched in the sub-layer of $Pt_{75}Ni_{25}$ or $Pt_{75}Re_{25}$ nanoparticles. Even better, the extent of enrichment is controllable by varying the nanoparticle size. It is widely believed that modification of the electronic structure of Pt by Ni (or Re) atoms is a major reason why alloying enhances catalytic performance for Pt-bimetallic surfaces. Therefore, our study points out that controlling the nanoparticle size can tailor the electronic structure of Pt in the nanoparticle surfaces, besides varying the type of alloying element and the overall composition.

Table I. Atomic concentrations of Pt atoms in the outermost layer (denoted C_1), the second layer (denoted C_2), the third layer (denoted C_3), and the remainder (denoted C_{core}) of cubo-octahedral $Pt_{75}Ni_{25}$ nanoparticles at T=600 K.

Number of atoms	C_1	C_2	C_3	C_{core}
586	97	44	75	59
1289	99	48	78	62
2406	99	55	75	64
4033	99	58	74	67

Table II. Atomic concentrations of Pt atoms in the outermost layer (denoted C_{surf}) and the core part (denoted C_{core}) of cubo-octahedral $Pt_{75}Re_{25}$ nanoparticles at T=600 K.

Number of atoms	C_{surf}	C_{core}
586	97	55
1289	98	61
2406	99	64
4033	99	66

CONCLUSIONS

In this work, we have investigated the segregation of Pt atoms to the surfaces of fcc $Pt_{75}Ni_{25}$ and $Pt_{75}Re_{25}$ cubo-octahedral nanoparticles. To this end, we first developed MEAM potentials for Pt-Ni and Pt-Re alloys based on experimental and first principles calculation results. Our MEAM potentials can reproduce most of the available results for the elemental Pt, elemental Ni, elemental Re, and intermetallic Pt-Ni and Pt-Re compounds. More importantly, they lead to surface segregation phenomena agreeing with experimental measurements for Pt-Ni and Pt-Re alloys. Using the Monte Carlo simulation method, we determined the equilibrium structures and further evaluated the segregation profiles for fcc $Pt_{75}Ni_{25}$ and $Pt_{75}Re_{25}$ cubo-octahedral nanoparticles. Our results indicate that (1) the $Pt_{75}Ni_{25}$ nanoparticles form a surface-sandwich structure: the Pt atoms are enriched in the outermost and third layers, while the Ni atoms are enriched in the second layer; (2) the equilibrium $Pt_{75}Re_{25}$ nanoparticles adopt a core-shell structure: a Pt-enriched shell surrounding a Pt-deficient core. Moreover, we found that the Ni or Re atoms are enriched (higher than overall composition) in the sub-layer of $Pt_{75}Ni_{25}$ or $Pt_{75}Re_{25}$ nanoparticles and the degree of enrichment varies with nanoparticle size. This implies that the nanoparticle size is an important parameter governing the catalytic properties of Pt-bimetallic nanoparticles.

ACKNOWLEDGMENTS

We are grateful to Dr. A. Canning and Dr. J. An for assistance in using the PARATEC code. This work was supported by the Office of Science, Materials Sciences Division, of the U.S. Department of Energy under Contract Nos. DE-AC03-76SF00098 at LBNL and W-7405-ENG-36 at LANL. The computations were carried out at the National Energy Research Scientific Computing Center (NERSC), which is operated by LBNL for the U.S. Department of Energy.

REFERENCES

1. N.M. Marković and P.N. Ross, Surf. Sci. Rep. **45**, 117 (2002).
2. M.I. Baskes, Phys. Rev. B **62**, 2727 (1992).
3. M.I. Baskes and R.A. Johnson, Modell. Simul. Mater. Sci. Eng. **2**, 147 (1994).
4. M.S. Daw and M.I. Baskes, Phys. Rev. B **29**, 6443 (1984).
5. G. Wang, M.A. Van Hove, P.N. Ross, and M.I. Baskes, "*Monte Carlo simulations of segregation in Pt-Ni catalyst nanoparticles*", in preparation.
6. G. Wang, M.A. Van Hove, P.N. Ross, and M.I. Baskes, "*Monte Carlo simulations of segregation in Pt-Re catalyst nanoparticles*", J. Chem. Phys., submitted.